Forum Acusticum 2011 - Aalborg - Denmark

Waveguide-Finite-Element based parameter study of car tyre rolling losses

Carsten Hoever, Patrick Sabiniarz, Wolfgang Kropp
Division of Applied Acoustics, Chalmers University of Technology, Gothenburg, Sweden.

Summary
Low rolling resistance and a low noise level are two characteristics of a car tyre which are often seen as conflicting with each other. Simultaneously, there is an increased demand for improvement in both fields due to legislative changes. Due to the fact that there is little to no detailed information available on the relation between rolling resistance and acoustical behaviour of car tyres, an in-depth investigation of this subject seems to be desirable. In a first step, a Waveguide-Finite-Element-Model (WFEM) of a car tyre is combined with a non-linear 3D contact model to calculate the resulting contact forces between tyre and road surface. This can be used to make a detailed prediction of the tyre vibrations. For steady state rolling the input power into the tyre at the tyre-road interface gives the rolling resistance in terms of dissipated power. This includes detailed information on frequency and wave order distribution of dissipation. Using a parameter study, it is evaluated how the rolling resistance is affected by material properties or the tyre design.

PACS no. 43.20.Mv, 43.40.At

1. Introduction

In the year 2006 the fuel consumption in the road transportation sector was responsible for 23 % of the CO_2 emissions in the European Union (EU) [1] with absolute emission values remaining constant or even increasing since 1990. For cars powered by classical combustion engines, about 30 % of the CO_2 emissions (in form of fuel consumption) are due the rolling resistance [2] and it is believed that a 10 percent reduction in average rolling resistance [. . .] promises a 1 to 2 percent increase in fuel economy [3]. At the same time, road traffic noise continues to pose a severe problem for huge parts of the population. Within the EU, for example, it is estimated [4] that about 210 million people are regularly exposed to road traffic noise levels exceeding the WHO guideline value for outdoor sound levels of 55 dB(A) and about 54 million people to road traffic noise levels exceeding 65 dB(A). A new EU wide labelling scheme for tyres [5], which includes (simplified) information about both the rolling resistance as well as the external rolling noise, aims at raising the public awareness for these topics. Yet, there is little to no detailed information available on the relation between rolling resistance and rolling noise generation of car tyres besides empirical data based on measurements. About 80 % to 95 % percent of rolling losses can be attributed to hysteretic losses in the tyres [6]. Most of the dissipation is related to deformation of the rubber material in the tread, hence possible ways of reducing the rolling resistance are changing the tread geometry, the rubber compound or reducing the thread thickness [6]. Any change, however, does not only affect rolling losses, but also other important aspects like wear, traction or noise generation. Knowledge about how the hysteretic losses are linked to the vibrational behaviour (e.g.
in terms of dominant frequencies or wave orders) can help to make design decisions for tyres with a low rolling resistance. Accordingly, an in-depth investigation of this relation seems to be desirable. In a first step, an existing waveguide finite element tyre model [7] is combined with a 3D contact model [8], to give the vibrational behaviour of the tyre when rolling on a real road. Rolling losses can then be directly calculated as input power into the tyre. Due to the nature of the tyre model, detailed information about frequency and wave order distribution of rolling losses can be obtained. A parameter study is conducted to evaluate how different material properties or the tyre design affect rolling resistance. It is not the goal to calculate exact values for the dissipated energy. The main reasons are the problem of obtaining accurate reference values for the specific tyre being modelled as well as the expected changes in material data during rolling due to temperature changes, which are not available in a qualitative form. As shown in [9], measured absolute values for rolling resistance can differ

significantly depending on the type of measurement device which is used. Accordingly, the aim is to obtain absolute values which are in a reasonable range and emphasise on the relative differences in dissipation between parameter combinations.

2. Fundamentals of rolling resistance and prediction methods

Generally, rolling resistance is defined as the mechanical energy converted into heat for a unit distance travelled [10], with a unit of J/m. Traditionally, this has been associated with a drag force of unit N opposing the direction of motion. Since the more general energy based definition seems to be more appropriate within the scope of this study, it will be used in the following. This also allows the use the term *rolling loss* as an equivalent expression for *rolling resistance*. The majority of the rolling losses can be attributed to hysteresis. During rolling, the tyre material is periodically deformed. Due to the viscoelastic properties of the rubber compound, in each cycle not all of the stored elastic energy can be regained, instead a part of it is dissipated. The main cause of deformation for a rolling tyre is the flattening of the contact patch. This leads to a propagation of disturbances inside the tyre structure as waves in a variety of different mode shapes and orders, ultimately leading to dissipation. How dissipation is distributed among different wave orders is one of the areas of interest for this study. A good summary of existing literature on the evaluation of rolling losses can be found in [3]. For the sake of brevity, only a few models are mentioned in the following. Hall and Moreland [11] and Lin and Hwang [12] calculate the dissipation based heat distributions inside a rolling tyre. Yam et al. [13] base their work on experimental modal analysis data. Stutts and Soedel [14] use a stationary tension band on an elastic foundation to calculate the rolling resistance from the deflection in the contact zone. Recently, Lopez [15] has presented a procedure in which the contributions of the large steady state tyre deflection and the road-tyre texture related tyre vibrations are calculated independently and then superposed. The work of Fraggstedt [9] is the basis for this analysis. He uses a waveguide finite element model (WFEM) of a rolling tyre to calculate the dissipated power. Frequency and wave order distributions are shown as well as individual element contributions to the overall dissipation. However, a detailed analysis of the results is missing and it is never investigated how changes in tyre parameters affect the dissipation.

3. Review of existing tyre models

Since the mid-1960s, a variety of different models have been developed, aiming at simulating the dynamic response of tyres. They range from analytical models, based on coarse simplifications to highly sophisticated numerical models, accounting for the detailed physical properties of tyres. In the following, a selection of tyre models found in the open scientific literature is reviewed. A very common approach is to model the tyre as some kind of (pretensioned) ring or plate structure on an elastic foundation. One of the first models was presented by Böhm in [16] and a few examples for the many, more and more refined, variations which later were presented include [17], [18] or more recently [19]. Although these models are simple and fast they generally capture the dynamic behaviour only well within a certain frequency region. The rapid development of computer capacity during recent decades has made it possible to perform detailed modelling of tyres using the finite element method (FEM). A number of examples [20] and [21]. Generally, FEM models, although flexible and capable of giving insight into local properties, suffer from high requirements on computer capacity and need for detailed input data. Waki et al. [22] presented a model based on an approach in which the tyre is considered as a waveguide along the circumferential direction. Initially, a short section of the waveguide is modelled using standard finite elements. A periodicity condition is then applied. This results in an eigenvalue problem from which the dispersion properties and cross-section modes are obtained. A similar approach was presented by Nilsson [23] who modelled the tyre based on the waveguide finite element method (WFEM) which combines an FE approach with wave propagation assumptions along the tyre circumference. A modified version of Nilsson's model has also been presented in [9] and lately in [7]. By utilising the waveguide properties of the tyre, the computational burden is significantly reduced compared to traditional FEM. Also the wave characteristics are more directly captured than with the FEM. Some details of the model will be described in the Sec. 4.1.

4. The tyre model

4.1. Waveguide finite element modelling

The waveguide finite element model of the tyre being used in this study is, apart from some small changes, identical to the the one previously described in [7]. It is modified version of the model presented in [9]. In the following a short overview of WFEM is given.

A waveguide is a system which has constant geometrical and material properties along one, typically long dimension, along which the motion can be described conveniently by a set of propagating waves with the right set of boundary conditions. In this sense a tyre is a waveguide for which the motion along the circumferential dimension can be described by a set of waves fulfilling a periodicity condition $\mathbf{u}(\phi) = \mathbf{u}(\phi \pm 2\pi)$, where $\mathbf{u}$ is the tyre displacement.

In WFEM the waveguide property is used in conjunction with conventional two-dimensional finite element modelling of the waveguide cross-section, i.e. in a cylindrical coordinate system the displacement component u_i for a point (r, x, ϕ) is given by (time dependency $e^{-j\omega t}$ dropped in the following)

$$u_i(r, x, \phi) = \mathbf{N}(r, x)\mathbf{v_i}(\phi) \quad i = r, x, \phi\,. \tag{1}$$

Herein, $\mathbf{N}$ is a vector of cross-sectional FE shape functions while $\mathbf{v_i}$ represents the corresponding nodal degrees of freedom. Thus, only the displacement dependance on the cross-sectional coordinates is approximated using FE modelling, while the nodal displacements are functions of the angular coordinate ϕ. Hence, they depend on the assumed wave propagation along this dimension. It has been shown [9] that based on Eq. (1), a set of coupled ordinary differential equations is obtained:

$$\left[-\mathbf{A}_{11}\tfrac{\partial^2}{\partial\phi^2}+(\mathbf{A}_{01}-\mathbf{A}_{10})\tfrac{\partial}{\partial\phi}+\mathbf{A}_{00}-\omega^2\mathbf{M}\right]\mathbf{v}(\phi)=\mathbf{f}(\phi)\,. \tag{2}$$

The generalised stiffness matrices $\mathbf{A}_{nm}$ and the mass matrix $\mathbf{M}$ are derived from the tyre's potential respectively kinetic energies and $\mathbf{f}$ is the generalised force vector describing the external load. By setting $\mathbf{f} = 0$ the homogeneous case is obtained, for which solutions are given by exponential functions of kind

$$\mathbf{v}(\phi) = \hat{\mathbf{v}}e^{i\kappa\phi}\,. \tag{3}$$

These can be physically interpreted as waves of cross-sectional mode shape $\hat{\mathbf{v}}$ travelling along the circumferential direction with polar wavenumber κ. Inserting (3) into (2) results in an eigenvalue problem which can be solved to get the eigenfrequencies and mode shapes for a specific polar wave number. The forced response case can e.g. be solved by means of an assumed mode procedure as described in [9].

4.2. Modelling of rolling contact

The model for the contact between the rolling tyre and the road surface is based on 3D model described in [8]. It accounts for the radial contact forces which are due to the indenting of the road roughness into the tyre tread. To get accurate results, three-dimensional roughness data is necessary, i.e. it is not sufficient to include only one roughness track along the circumferential direction, the roughness variation along the lateral direction has also to be accounted for. Moreover, the tyre vibrations are a function of the contact forces while, at the same time, the contact forces also are a function of the tyre vibrations. This nonlinearity leads to a formulation in the time domain. For a specific contact patch and radial contact forces, the dynamic problem can be described by the following system of equations

$$\mathbf{F}(t) = \mathbf{C}^{-1}\,\mathbf{\Delta y}(t) \tag{4a}$$

$$\mathbf{\Delta y}(t) = y_0(t) + \mathbf{k_r}(t) + \boldsymbol{\xi}(t) - \mathbf{k_t}(t) \tag{4b}$$

$$\xi_n(t) = \sum_m F_m(t) * g_{m,n}(t)\,, \tag{4c}$$

where $\mathbf{F}(t)$ are the contact forces for all contact points, $\mathbf{C}$ is an influence matrix obtained from an elastic-half space representation of the tyre tread and $\mathbf{\Delta y}(t)$ is the tread deformation. $y_0(t)$ denotes the centre position of the rim whereas $\mathbf{k_r}(t)$ and $\mathbf{k_r}(t)$ describe the profile of the road roughness and the tyre and are obtained from surface scans. Finally, $\boldsymbol{\xi}(t)$ is the dynamic displacement of the tyre structure around the neutral line. Its components $\xi_n(t)$ are given by the convolution of the contact force $F_m(t)$ at position m, with the Green's function $g_{m,n}(t)$. The Green's functions can be directly obtained from the tyre's WFE model. The set of equations (4) is finally iteratively solved for every time step.

In order to decrease the computational burden and due to the nature of the WFEM mesh, different levels of discretisation are used for the road roughness and tyre profiles. Whereas the discretisation of the road and tyre profiles is very fine to capture even small variations, the discretisation of the contact patches on the tyre structure is coarser, i.e. the contact forces are integrated locally to excite specific solid elements of the tread structure. The validity of this approach is shown in [8]. After transformation to the frequency domain the contact forces are rotated around the tyre to give the response in the Lagrangian coordinate system.

4.3. Power dissipation

Due to energy conservation the energy going into the tyre must be equal to the dissipated energy under steady-state rolling. Because the rolling is assumed to be a continuous process, it is more appropriate to speak of dissipated power instead of dissipated energy. The time-averaged input power into the tyre is given as

$$P = \frac{1}{T}\sum_i \int_0^{2\pi}\int_0^{T} F_i(t,\phi)\,\frac{\partial v_i(t,\phi)}{\partial t}\,dt\,d\phi\,. \tag{5}$$

Herein, F_i and $\partial v_i/\partial t$ denote the contact force respectively tyre velocity for the lateral contact track i.

4.4. Modelling details

In this study a model similar to that of the 205/55R16 tyre as previously described in [7] is used. It consists of 29 deep shell elements which constitute the sidewalls and the belt, and 13 two-dimensional solid elements

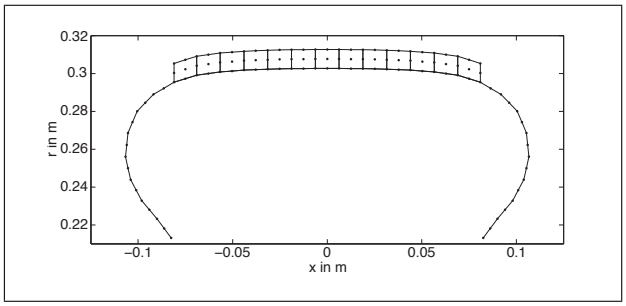

Figure 1. Mesh of the modelled 205/55R16 tyre.

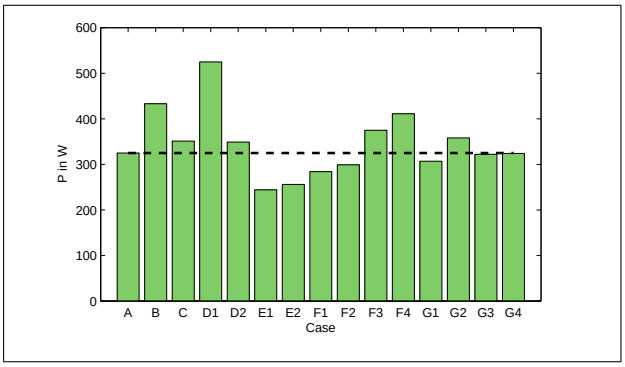

Figure 2. Dissipated power for all cases. (−−) dissipation of original configuration A.

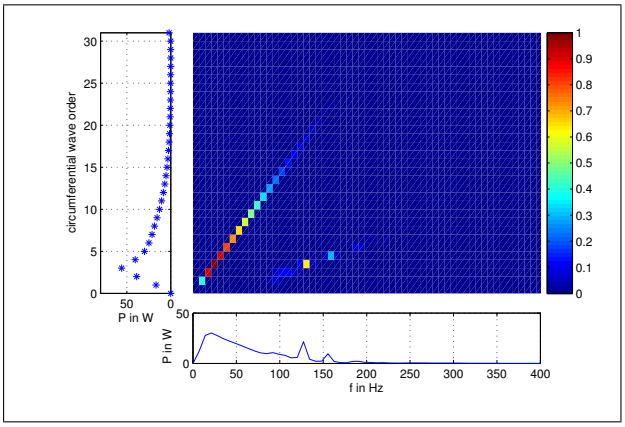

Figure 3. Dissipated power as a function of frequency and circumferential wave order for configuration A. Colour is re. maximum of plot.

which are used to model the rubber tread. A detailed description of both element types can be found in [9]. The resulting cross-sectional tyre mesh can be found in Fig. 1. In [9] a mesh of similar size is shown to give sufficient results up to at least 1000 Hz, which was also proven by a small convergence study. Along the tyre circumference, 512 response positions are evaluated. Aside from omitting tread groves, the air cavity is not explicitly modelled (but the resulting pre-tension is included). Also the wheel is not included explicitly in the simulations, instead the tyre motion at the bead is blocked. Most of the required tyre data is based on an provided input deck and a subsequent parameter tuning to match measurements. In the following a brief overview of the input parameters is given, for a detailed description see [7]. For the isotropic solid tread elements a Young's modulus E of roughly 20 MPa and a Poisson's ratio ν of 0.49 are assumed. The necessary stiffnesses and pretensions for the shell elements are directly taken from the input deck (with small adaptions as mentioned in [7]). Damping is based on a stiffness-proportional model. For the shell elements the loss factor η assumes a value of 0.05 below the cut-on frequency of the first symmetric belt bending mode and 0.15 above it with a transition region extending from roughly 280 Hz to 370 Hz. For the solid elements representing the highly damped rubber, the loss factor is set to $\eta = 0.25$. A driving speed of 50 km/h and a loading of 3415 N are assumed. The tyre surface is considered to be slick and the road roughness profile is based on a scan of 15 lateral tracks of an drum-mounted ISO 10844 road surface. The obtained frequency resolution is 7.1 Hz.

4.5. Parameter study

An overview of the conducted simulations can be found in Tab. I. Therein, the setup described in Sec. 4.4 is denoted as configuration A. Configuration B changes speed and load to match the simulations presented in [9] and configuration C uses a surface scan of a rough road instead of the ISO surface scan. In each of the remaining parameter sets D to G a certain aspect of the tyre's physical properties is changed, namely the damping (D), the inflation pressure (E), the sidewall stiffness (F) and the overall weight respectively the mass distribution (G). It shall be noted that at this stage of the study the aim is not at keeping parameter variations necessarily within limits which are realistic from an engineering point of view. Instead partly extreme changes are made to better understand how certain aspects of the tyre construction affect the rolling loss.

5. Results

In the following some preliminary results of the parameter study are given. Fig. 2 shows the total dissipated power for all simulated cases. For the original configuration A the total dissipated power is calculated as 325 W. Fig. 3 depicts the distribution of the dissipated power over frequency respectively circumferential wave order. All of the relevant dissipation occurs below 200 Hz, with a wide maximum around 21 Hz and two narrow maxima at 127 Hz and 156 Hz. In the wave order domain, dissipation is concentrated at wave orders 2 to 4. Wave orders 15 and higher only contribute to a very small extent to the dissipation. Taking the combined wave-order-frequency plot in Fig. 3 into a account, two distinct dissipation patterns can be identified. In [7] an analysis of the free

Table I. Calculated cases for the parameter study.

Case	Description
A	Original parameters as described in Sec. 4.4.
B	Original tyre data. 80 km/h, static load 2943 N.
C	Original tyre data. Rough road surface.
D1/2	All loss factors multiplied by 2/0.5.
E1	Pretension multiplied by 2. Young's modulus tread multiplied by 0.5 to keep contact area size constant.
E2	All pretension values multiplied by 1.5.
F1/2/3/4	All sidewall Young's moduli multiplied by 2/1.5/0.75/0.5.
G1/2	All densities multiplied by 1.25/0.75.
G3	Changed mass distribution: Heavier sidewalls. Total tyre weight kept constant.
G4	Changed mass distribution: Heavier tread centre. Total tyre weight kept constant.

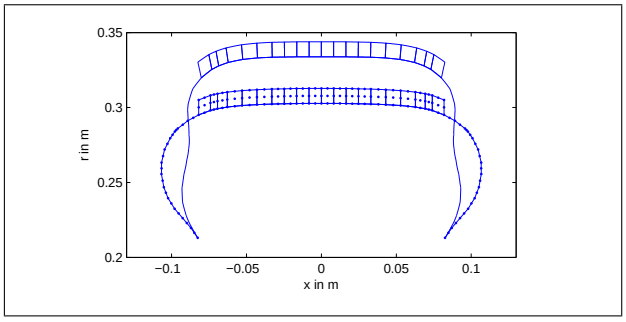

Figure 4. Cross-sectional mode shape for waves of type 127 Hz/order 3 and 156 Hz/order 4. Note: Shown mesh is not the one used in this study.

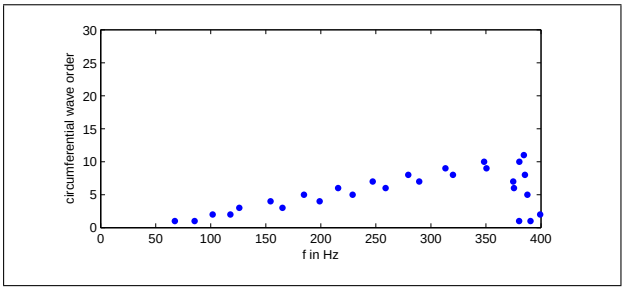

Figure 5. Dispersion relations. Each dot represents a free response solution for the undamped tyre.

wave field on a tyre was conducted. The results obtained there reveal that the dissipation maxima at 127 Hz and order 3 and 156 Hz and order 4 belong to a group of waves which are characterised by a radial motion of the whole tread region as shown in Fig. 4.

However, the majority of dissipation in Fig. 3 can be attributed to a straight line running from the coordinate origin to around wave order 20 and 140 Hz. In [7] this region could not be associated with any free wave motion in the tyre, see also Fig. 5. Instead, this feature is governed by excitation properties. Based on the tyre circumference and the rolling speed, the fundamental excitation frequency is 7.1 Hz and together with the higher harmonics this results in the characteristic straight line.

The distribution of dissipation along this line seems to be mainly governed by the size of the contact patch. A typical contact patch length of around 10 cm corresponds to roughly an eighth to a quarter of the wave lengths of the dominating wave orders 2 to 4. Hence, strong excitation can be assumed. Contrary, for wave orders 10 and higher the wave length becomes equal to or smaller than the contact length which means that the contribution of these orders to the global deformation of the tyre structure in the contact area is rapidly decreasing. Cases B and C show the expected negative influence of speed respectively a rougher road surface on the rolling resistance. Moreover, case B can be used for comparison with the results obtained by Fraggstedt in [9] for almost identical conditions, albeit for a different tyre. The difference is around 10 % and can be attributed to the different tyre and non-identical road surface scans. The results of the changes in inflation pressure (E), and sidewall stiffness (F), are as expected with an increased pressure respectively higher sidewall stiffness leading to a reduction in rolling resistance. The highest reduction of 25 % is achieved by doubling the inflation pressure, but even an increase of only 50 % still results in about 21 % lower rolling losses. The doubling of the loss factor in case D1 leads to the expected high increase of dissipation but what is remarkable is that the dissipation also increases for case D2 where the loss factors are decreased. A possible explanation might be given by Fig. 6 which shows that lower loss factors lead to a lower dissipation in the low frequency regions but results in considerably more and higher narrow peaks between 100 Hz and 270 Hz which relate to free wave motion on the tyre. A possible explanation is that a reduction of damping leads to lower losses in the tread region during the actual contact and hence a higher excitation of free waves on the tyre which, even though they are less damped, contribute significantly to the dissipation in the long run. A similar effect can be seen for

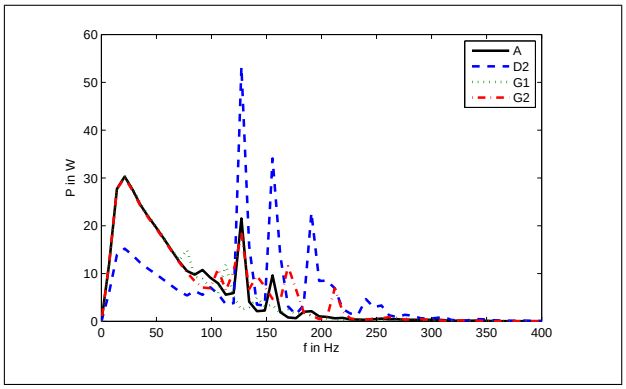

Figure 6. Comparison of dissipated power in the frequency domain for cases A, D2 (lower damping), G1 (higher mass) and G2 (lower mass).

the changed tyre mass in cases G1 and G2. Fig. 6 reveals that the low frequency behaviour is identical to the original tyre and all changes in dissipation can be attributed to the higher frequency regions characterised by free wave propagation. The change of mass distribution in G3 and G4, finally, does not lead to any significant changes in rolling resistance and is hence not further commented upon.

6. CONCLUSIONS

A way is shown how to assess rolling losses based on the input power calculations for an existing waveguide finite element model of a car tyre which is coupled with a three-dimensional model for rolling contact. The estimated total rolling loss is comparable to values found in the literature and detailed examination of the frequency and wave order content reveals that for normal driving speeds a major part of the rolling losses can be attributed to the forced excitation of the tyre in regions below the cut-on frequencies of the lowest circumferential wave orders. Additionally there is a limited contribution of certain propagating waves in frequencies up to 300 Hz. In general, rolling resistance seems to be a low-frequency, low wave order problem. The parameter study mostly reveals expected changes due to changes in the tyre construction. The influence of changed damping and overall tyre weight, which seem to affect the distribution of losses between low frequency regions without free wave propagation and higher frequency regions with free wave propagation will be the topic of further investigations in the future. For this the model will be extended to allow the calculation dissipation distribution over the individual elements of the tyre mesh.

Acknowledgement

The work presented in this paper has been financially supported by the European Commission research project *Green City Car*, SCP8-GA-2009-233764.

References

[1] Annual EC greenhouse gas inventory 1990–2006 and inventory report 2008. Report No 6/2008, EC, EPA, 2008.

[2] Final Report SI2.408210 Tyre/Road Noise - Vol. 1. FEHRL, 2006.

[3] Tires and passenger vehicle fuel economy. Report 286, Transportation Research Board, 2006.

[4] L. den Boer, A. Schroten: Traffic noise reduction in Europe. CE Delft, 2007.

[5] Regulation (EC) 1222/2009. Europ. Parliament, 2009.

[6] The pneumatic tire. U.S. Departm. of Transp., 2006.

[7] P. Sabiniarz: Modelling the vibrations on a rolling tyre and their relation to exterior and interior noise. PhD thesis, Chalmers Univ. of Techn., Gothenburg, 2011.

[8] F. Wullens: Excitation of tyre vibrations due to tyre/road interaction. PhD thesis, Chalmers Univ. of Techn., Gothenburg, 2004.

[9] M. Fraggstedt: Vibrations, damping and power dissipation in car tyres. PhD thesis, Royal Inst. of Sciences, Stockholm, 2008.

[10] ISO 18164:2005.

[11] D. Hall, J. Moreland: Fundamentals of rolling resistance. Rubber Chem. and Techn. **74** (2001) 525-539.

[12] Y. Lin, S. Hwang: Temperature prediction of rolling tires by computer simulation. Math. and Comp. in Sim. **67** (2004) 235-249.

[13] L. Yam et al.: Study on tyre rolling resistance using experimental modal analysis. Int. Journ. of Veh. Design **30** (2002) 251-262.

[14] D. Stutts, W. Soedel: A simplified dynamic model of the effect of internal damping on the rolling resistance in pneumatic tires. Journ. of Sound and Vibr. **155** (1992) 153-164.

[15] I. Lopez: Influence of material damping on the prediction of road texture and tread pattern related rolling resistance. Proc. ISMA 2010, 4039-4052.

[16] F. Böhm: Mechanik des Gürtelreifens. Archive of Applied Mechanics **35** (1966) 82-101.

[17] K. Larsson, W. Kropp: A high-frequency three-dimensional tyre model based on two coupled elastic layers. Journ. of Sound and Vibr. **253** (2002) 889-908.

[18] Y. Kim, J. Bolton: Modelling tyre treadband vibration. Proc. Internoise 2001.

[19] P. Kindt et al.: Development and validation of a three-dimensional ring-based structural tyre model. Journ. of Sound and Vibr. **326** (2009) 852-869.

[20] L. Kung et al.: Free vibration of a pneumatic tire-wheel unit using a ring on an elastic foundation and a finite element model. Journ. of Sound and Vibr. **107** (1986) 181-194.

[21] M. Brinkmeier et al.: A finite element approach for the simulation of tire rolling noise. Journ. of Sound and Vibr. **309** (2008) 20-39.

[22] Y. Waki et al.: Free and forced vibrations of a tyre using a wave/finite element approach. Journ. of Sound and Vibr. **323** (2009) 737-756.

[23] C.-M. Nilsson: Waveguide finite elements applied on a car tyre. PhD thesis, Royal Inst. of Sciences, Stockholm, 2004.